Geodesy and Geodynamics 9 (2018) 57–66

Contents lists available at ScienceDirect

Geodesy and Geodynamics

journal homepages: www.keaipublishing.com/en/journals/geog;
http://www.jgg09.com/jweb_ddcl_en/EN/volumn/home.shtml

Seismic-gravimetric analysis of the subducted Nazca plate 1 between 32°S and 36°S

Lujan Eckerman [a, *], Alejo Agüero [b], Silvana Spagnotto [a, c], Patricia Martinez [c, d], Silvina Nacif [c, d]

[a] Universidad Nacional de San Luis, San Juan, Argentina
[b] YPF S.A. San Juan, Argentina
[c] CONICET (National Scientific and Technical Research Council), San Juan, Argentina
[d] Instituto Geofísico Sismológico Volponi – 5 Universidad Nacional de San Juan, Argentina

ARTICLE INFO

Article history:
Received 11 May 2017
Received in revised form
1 August 2017
Accepted 4 August 2017
Available online 19 December 2017

Keywords:
Subducted Nazca plate seismicity
Intermediate earthquakes
Gravimetric profile

ABSTRACT

The study region is seismically and tectonically characterized by the angle variations in the subduction of the Nazca plate. The results obtained from earthquakes location between 32° and 36°S latitude and 67°–71°W longitude are presented in this work. The presence of a wedge of asthenospheric materials and the partial or total eclogitization of the subducted Nazca plate and its relation with isostatic cortex models published was analyzed. In addition, a gravimetric profile obtained from gravity forward modeling is presented at 33.5°S, proposing a new configuration at depths for the main tectonic components: Nazca plate, asthenospheric wedge and South American plate. Also, a new density scheme using recently published velocity models was obtained.

1. Introduction

The Nazca plate subducts below the South American plate along the ocean trench of Chile and Peru, at a velocity of 6.7 ± 0.2 cm/year according to GPS measurements [1]. The plate convergence direction is consistent with horizontal displacements triggered by earthquakes in the megafault. Tong et al. [2], Vigny et al. [3] and Delouis et al. [4] obtained displacements that range from 3.3 to 5 m in the same direction.

Also, the region is seismically and tectonically characterized by angle variations at which the oceanic plate subducts below the continental plate [5–7]. North of 32.5° S, the plate subducts flat at 100 km deep for 300 km towards the east. In the south of this latitude the plate subducts with a normal angle of 27° at approximately 170 km deep [8,9]. The study area was divided into three regions with different subduction angles obtained from Wadati-Benioff curves (Fig. 1).

In particular, the seismicity of intermediate depths (~50–~300 km deep) has its origin in different processes in subducted Nazca plate [11]. For the depths presented here, Kirby et al. [12] and Meade and Jeanloz [13], suggest dehydration processes, and Hacker et al. [14], using thermo-petrological models, relate metamorphic dehydration reactions to seismicity, proposing this phenomena as the origin of intermediate earthquakes.

Oceanic lithosphere flexure causes normal fault in the outer rise faults and deep hydration by water infiltration into the crust fragile sector [15]. The slab flexure creates conjugated extensional faults for each of them. The strikes and dips of focal mechanism suggest reactivation of outer rise faults at intermediate depths [16,17]. The bathymetries performed on the Chilean coast [18,19] show three different structural patterns: fault reactivation of the ocean opening with a strike angle of 145°, new faults formed by the flexure and parallel to the trench, and faults parallel to Juan Fernandez Ridge with strike of 60°.

* Corresponding author.
E-mail address: lujan.eckerman@gmail.com (L. Eckerman).
Peer review under responsibility of Institute of Seismology, China Earthquake Administration.

Production and Hosting by Elsevier on behalf of KeAi

https://doi.org/10.1016/j.geog.2017.08.002

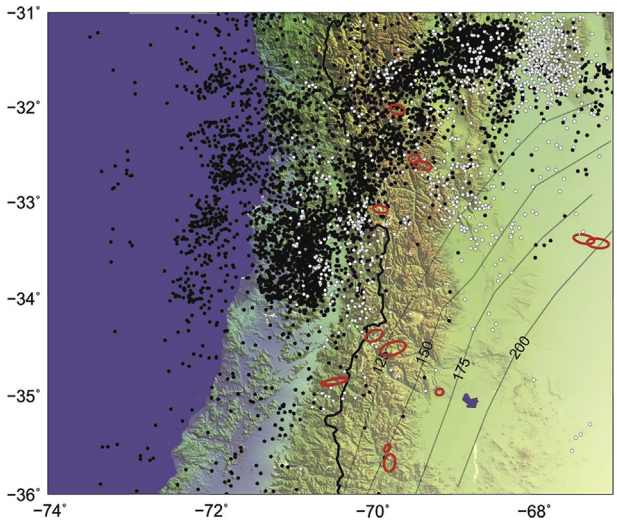

Fig. 1. Study area: points indicate the NEIC/USGS seismicity, in black morphology of subducted Nazca from Mulcahy et al. [10], studied earthquakes projected horizontally in red error ellipses here.

In this paper, we calculate the stress tensor and make a density model, contributing new knowledge to understand the geodynamics of the subduction of the Nazca plate.

2. Tectonic environment

2.1. North sector

In the northernmost study region, the slab initially subducts with a normal angle up to 100 km deep and then remains horizontal for about 300 km to the east [7].

Kopp et al. [19] find subducted slab thicknesses of only 10 km and attribute buoyancy to the crust hydration and upper mantle of the slab. Gans et al. [20], using receiver functions, find thicknesses of 13–19 km. The Green's functions at the flat slab region, rotated according to the trajectory of the Juan Fernández Ridge, show a slab ripple, suggesting a small dip to the west around 69°W. They also find that the subducted crust is fractured by faults parallel to the trench, which they attributed to old structures of subducted plate or tectonic underplating caused by the coupling between the plates in the flat slab region. Pardo et al. [21] evaluate intermediate depth seismicity along the subducted Juan Fernández Ridge and report normal fault with the T axes along the slab and other strike-slip mechanisms with T axes with north-south component, which cannot be explained only by slab pull forces. They proposed the reactivation of preexisting faults in the oceanic crust near the subduction and outer rise zone due to the Juan Fernández Ridge subduction influence.

The regional stress tensor from Bilbao [22] reports shows $\sigma 1$ vertical (azimuth 149° and inclination 80°), whereas the $\sigma 3$ is almost horizontal and with orientation of NNW-SSE (azimuth 339° and dip 9.6°). The Bilbao [22] results indicate a clear influence of the raised sector of the subducted plate. It is important to point out that the referred tensor was obtained with the data from a reduced region around the flat slab.

The regional stress tensor solved by Pardo et al. [21] in the same sector, is similar but $\sigma 1$ and $\sigma 2$ are rotated [22]. The difference may be in that, when taking mechanisms located south of Bilbao [22], the influence of the slab pulls in the transition zone and it is more relevant. Additionally Salazar [23], Alvarado et al. [24] and Alvarado et al. [25], find the sigma $\sigma 1$ vertical in the horizontally subducting plate.

2.2. Central sector

This zone is located in the transition section where the Nazca plate changes from flat slab in the north of ~33°S to normal slab in the south of that latitude [9]. In the central sector Nacif [26], Spagnotto [27] and Nacif et al. [9] detect a decrease in seismicity at 120 km depth. This process can be explained as a product of the completion of the metamorphic process by dehydration and subsequent eclogitization taking place from ~100 to ~170 km deep [12]. Nacif et al. [9] consider that eclogitization process could have been the source of fluid release which originated from the magmatic activity that contributes to the formation of pleistocene volcanoes and now have little or no magmatic activity. This process also influenced the densification of the oceanic plate which produces a differential sink leading to have an angle greater than 27°.

On the other hand, in the plate, Spagnotto et al. [28] observed a rupture that penetrates the upper lithosphere mantle. In this study, two events are related when the second of them is entirely developed in the mantle breaking 40 km down. The fault plane generated by these two events has a strike and dip consistent with the outer rise faulting and for this reason, they reactivate at 120 km deep. In addition, the slip is consistent with the flexure and 20 stretching produced by the slab pull force.

2.3. South sector

Nazca plate subducts with a normal angle of 27° to a depth of 170 km [8,26]. In this area Burd et al. [29], using magnetotelluric data, identified two plume structures with significant electrical conductivity, one shallow asthenospheric towards West and another deep towards East. The first structure approaches the surface beneath the Caldera Payún Matrú and the Tromen volcano with west dip toward the subducted Nazca plate. The second structure, called DEEP (Deep Eastern Plume), approaches the surface approximately 100 km to the south and steeply deepens at 400 km deep to the east but always above the subducted slab.

A similar structure to DEEP had already been identified by Burd et al. [30], and had also been recognized by Ramos and Folguera [31], but in that study it was only interpreted as an indicator of current flow between mantle transition zone and surface crust. Lupari et al. [32] found earthquakes at anomalous intermediate depths (between 50 and 100 km deep) above the subducted Nazca plate.

Also Rojas Vera et al. [33], through the analysis of geophysical, geochemical and geochronological data, obtained the reconstruction of the Loncopue trough and its evolution from the Jurassic to the late Cretaceous-Eocene. The authors found a positive relief followed by a relaxation in two extensional stages. This scenario, characterized by a thinning of the crustal seismic thicknesses and relatively unusual heat flow areas, is discussed on the basis of below three main hypotheses:

- An increase of slab subduction slope after a shallow subduction scenery.
- A stretching of the co-seismic crust linked to large earthquake in the interplate subduction zone.
- A slab tearing associated with asthenospheric ascent.

3. Methodology

We use data of year 2001, from CHARGE (CHile Argentina Geophysical Experiment) recorded between November 2000 to May 2002. Seismic events (magnitude ≥ 3) located and reported by U.S. Geological Survey (NEIC-Catalog) were selected. The waveform data from Seismic Query (http://www.iris.edu/SeismiQuery/breq_

fast.phtml) were downloaded. Between 2012 and 2014 we added temporary experiment data from San Rafael Block (SRB) located in the backarc region of Malargüe, Mendoza Province, Argentina (Fig. 2).

The seismological processing was made within Seisan 9.1 [34,35] platform and the HYPOCENTER code was used (within Seisan) to obtain relocations and coda magnitudes (Mc). Two different one-dimensional velocity models were considered by Nacif et al. [9] and Spagnotto [27], for the northern and southern region respectively. To obtain focal mechanisms from P-wave first motion polarities we applied three different programs: HASH [36], FOCMEC [37] and FPFIT [38]. Additionally, the FaultKin 7.4.1 software was used to obtain the regional P and T axes.

With regard to the gravimetric study, the data was provided by the IGSV (Instituto Geofísico Sismológico F. Volponi) – Argentina. Data from different sources such as the IGN (Instituto Geográfico Nacional) – Argentina, the IFIR (Instituto de Física de Rosario) – Argentina, the IGSV, and the University of Leeds (England) was put into a unified database, namely IGSN 1971 (International Gravity Standardization Net 1971) [39]. The software used to perform data processing was Geosoft's Oasis Montaj. The charts of anomalies were calculated for the central sector of study using the international reference ellipsoid of 1967 (Geodetic Reference System 1967 (GRS67) [39]) and applying the free air corrections, Bouguer and topographic corrections. To perform the topographic correction it is necessary to have two models of digital terrain elevation: local one and regional one. These models were downloaded (http://www.ngdc.noaa.gov). An average density in the rocks was assumed to be 2.67 g/cm^3 [40], to a distance of 167 km. A Bouguer anomaly chart was obtained, gridded every 2.5 km with the least square method. To make gravimetric and seismological interpretations we applied filtering techniques, such as analytical continuation and trend surfaces (the 1st, 2nd and 6th order polynomial surfaces approximately representing regional anomalies).

In order to link the different anomalous sources with the gravimetric signal, a gravimetric model was performed along the AB profile at 33.5°S. This cross section with a length of 380 km in E–W direction cuts different geological structures of crustal domain.

The density model along the AB profile (Fig. 3) was calculated with the Bouguer anomaly using the GM-SYS program developed by Webring [41]. Gravity forward modeling denotes the computation of the gravitational field generated by some source mass distribution.

It was based on a simple five-layer model where the following was considered:

Upper crust ($\rho = 2.9$ g/cm^3)
Lower crust ($\rho = 2.9$ g/cm^3)
Upper mantle ($\rho = 3.3$ g/cm^3)
Nazca Plate ($\rho = 3.05$ g/cm^3)
Lower mantle ($\rho = 3.41$ g/cm^3)

All initial densities were established according to Nacif et al. [9] and Tassara et al. [42]. The obtained values were quite coincident with those globally recognized, such as Woollard [43], Introcaso, et al. [44], Gimenez et al. [45], Martinez et al. [46], etc. This simple model was modified to include a wedge of asthenospheric materials, lateral variation of densities in the continental crust (Chilenia and Cuyania) [47–49], and lateral variation of densities in the subducted Nazca plate since it sinks, dehydrates and densifies [50].

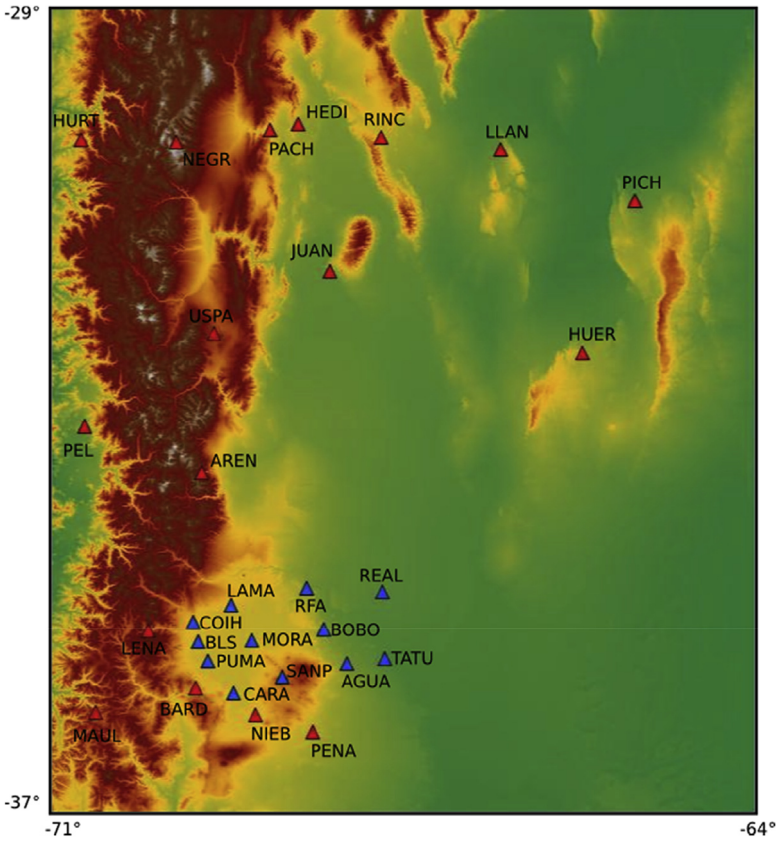

Fig. 2. Stations used in this work. Stations in red belonging to CHARGE; stations in blue belonging to SRB.

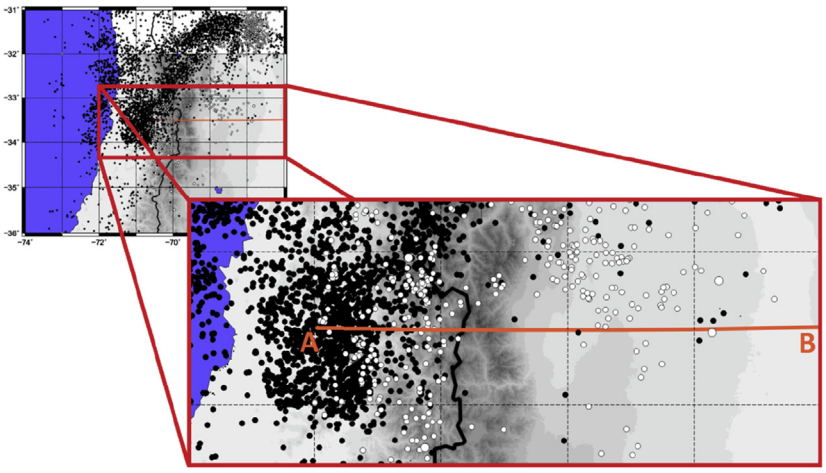

Fig. 3. Geographic location of gravimetric profile (orange line). It has a length of 380 km and extends in the W–E direction. NEIC/USGS catalog earthquakes (black and white dots) are also shown.

The response calculated from this initial model was adjusted by varying the geometry of the mentioned interfaces to achieve the model that best fits the observed data.

4. Results and discussion

A profile of subsurface densities was made for 33.5°S from a gravity forward modeling and adjusted a theoretical response with observed data. The density model (Fig. 4) extends for 380 km and includes lateral variation of densities in the Continental Crust (Upper and Lower) between the Chilenia and Cuyania terrains. There is also the representation of the subducted Nazca Plate (Oceanic Crust and Oceanic Mantle), the asthenospheric materials wedge, the base of the Lithospheric Mantle and the Asthenosphere.

It is important to note that the asthenospheric wedge materials in this study had not been taken into account in previous works for the latitude involved neither was the consideration of a Nazca plate densified by possible dehydration processes.

In Table 1, we show localizations, magnitude and focal mechanism obtained with polarities of first arrivals and amplitude relations of analyzed sixteen events.

We obtained three profiles, one in the north (32°–33°S), one in the center (33°–34°S) and a third one in the south (34°–36°S) (Figs. 5–7), on which the seismicity of the NEIC/USGS catalog and the ones studied in this work were plotted.

These locations are consistent with the morphology of the plate proposed by other authors [8,9]. We show two events in the profile at 33.5°S (Fig. 4), one located at 198.3 km and the other at 207.6 km deep, which indicates the existence of rigid slab at these depths. Pesicek et al. [51], using tomography, interpreted horizontal and vertical tearing of the slab at 38°S, but the transition from a horizontal to moderately subducting slab in the northern portion of the model is imaged as a continuous slab bend. We speculate that the tearing was most likely facilitated by a fracture zone in the descending plate or a continental scale terrain boundary in the overriding plate. Nacif and Triep [52] have suggested a similar break at least at those longitudes. This result contradicts with ours. On the other hand, Portner et al. [53] reported a plate hole in the northern sector. On the contrary, our gravimetric model is consistent with a denser plate with low water content (Fig. 4) and we see no evidence of broken plate. However small amounts of water added to the slab pull could be responsible for the earthquakes mentioned. The normal fault mechanism of 2011/12/24 earthquake seems consistent with this interpretation.

Table 1 shows the locations, depth error, rms and the number of stations used in each case. In Fig. 1 horizontal errors can be seen and it is clear that these are small. In all cases, the horizontal and vertical errors are approximately equal to those of the morphology or less. Relocated earthquakes did not show great variations with respect to the latitude and longitude given by NEIC/USGS, although the same did not happen with the depth.

The fault plane of the events corresponds to a west-dipping normal fault with strike and dip which are consistent with those of the outer ridge faults [54]. Thus, these events could be related to a preexisting fault originated in that environment and reactivated at 100 km deep. The slip is consistent with the bending produced by the slab pull. Spagnotto et al. [28] find evidence that two earthquakes at 32.5°S would be reactivations of the outer rise and be part of a fault that penetrates the mantle.

There may also be faults associated with current stresses, which is why other orientations also appear.

In order to analyze the plate stress state, considering the tectonic behavior in each one of them, the study area was separated into three regions: to the north, horizontal subduction, normal subduction in the center and in the most austral zone, in addition to normal subduction, the presence of a plume of asthenospheric material. Then the results were compared with those obtained by other authors.

In the northern area several authors calculated the regional stress tensor. If we compare the principal axes of the stress tensor obtained in this work for that region and those obtained by Bilbao [22], Salazar [23], Pardo et al. [21] and Alvarado et al. [25], we can observe that the position of the maximum principal stress axis (P) is almost vertical in all the studies (in this work it has some inclination towards the NE). However, the minimum main stress axis (T) presents more noticeable variations (Fig. 7). Bilbao [22] awarded the difference of the position of σ3, compared to that obtained by Pardo, since it also uses earthquakes in the back-arc Andean region, (between 30° and 32° and 65° and the coast). Salazar [23] calculates the P and T axes with events distributed between 31.3° and 34° and 67.5° and the coast. Bilbao [22] explains that the σ3 obtained in her work matches with the plate morphology in the most elevated horizontal section of the Nazca slab in subduction, suggesting that the flexural stresses of the plate in combination with its weight and buoyancy in the raised part would determine the occurrence of seismicity.

Our result is consistent with that of Alvarado et al. [25] (Fig. 8) and inconsistent with the average of Bilbao [22]- which was

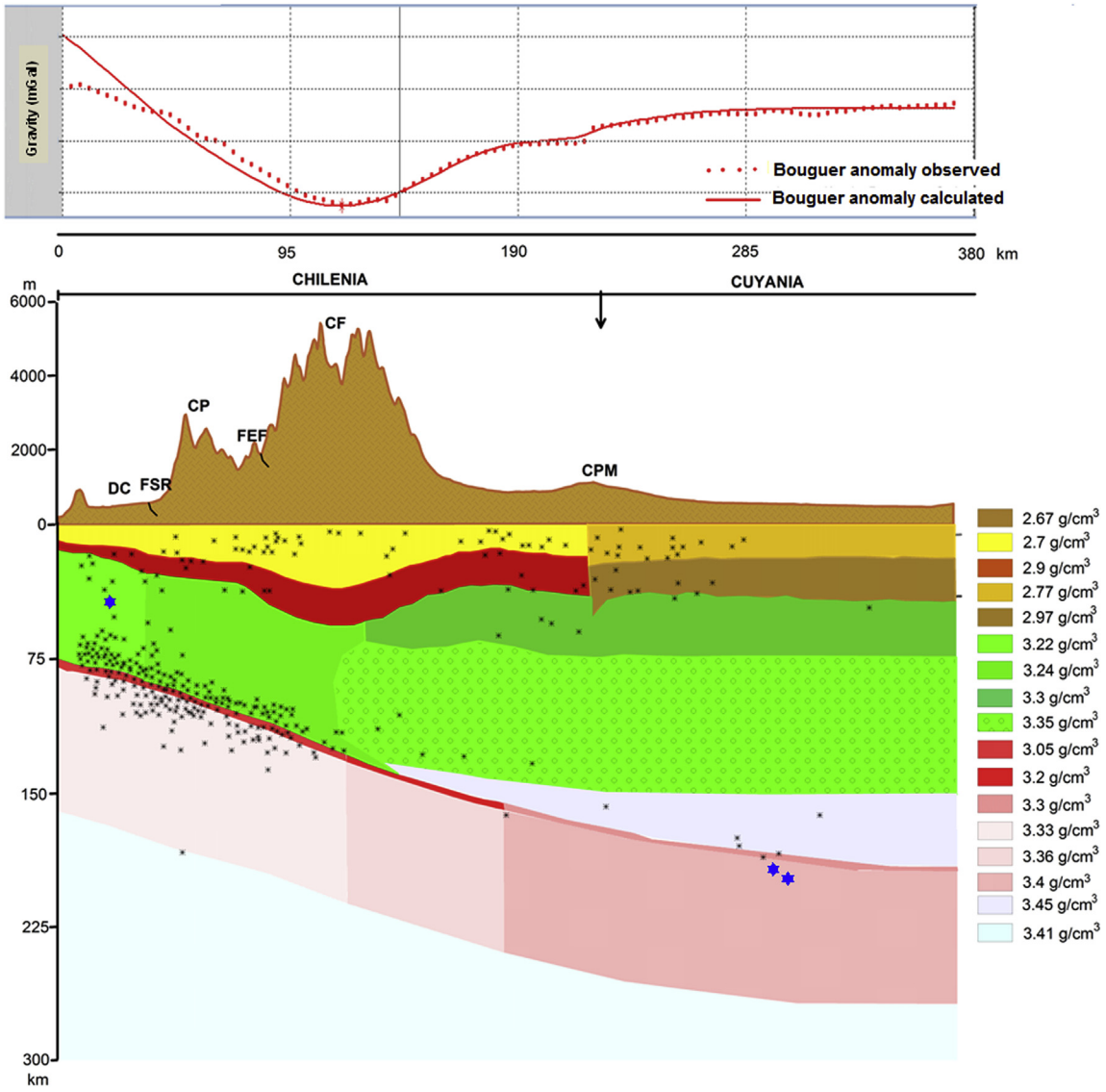

Fig. 4. Discontinuities of profile for 33.5°S: Bouguer anomalies (observed and calculated). There is a difference between them towards the west of the profile due to the fact that the Central Depression (DC), the San Ramón fault (FSR), or the El Fierro fault (FEF) have not been taken into account in the model. Neither have smaller intermontanas depressions. Below: Model of densities and earthquakes located in this work (in blue). The black spots are the events previously located and extracted from the NEIC/USGS catalog. References in letters: CF – Frontal Cordillera, CP – Main Cordillera, CPM – Cerro Pampa Muerto.

Table 1
Localization parameters, error in depth, magnitude and focal mechanisms. The used velocity models are indicated, Spagnotto [27] velocity model in gray and Nacif [9] velocity model in pink.

Date	Hour	Latitude (°)	Longitude (°)	Depth (km)	Depth error (km)	RMS of time residuals	Number of station used	Magnitude (Mc)	Focal mechanisms								
									HASH			FOCMEC			FPFIT		
									Strike	Dip	Rake	Strike	Dip	Rake	Strike	Dip	Rake
Jan. 7, 2001	02:52:47.00	−34.506	−70.004	125.9	7.8	0.7	13	4.1				24	88	−29			
Jan. 7, 2001	20:59:30.00	−34.836	−70.703	134.4	15.5	0.5	10	3.9	102	51	−139						
Apr. 18, 2001	09:29:07.20	−33.411	−67.708	207.6	20.3	1.1	15	3.9				55	40	−25			
June 20, 2001	10:45:28.40	−32.044	−69.699	133.1	15.7	1.2	16	4.0				94	54	−58			
June 23, 2001	22:19:37.30	−32.561	−69.766	126.1	7.4	1	17	3.9				219	59	−59			
Nov. 19, 2001	11:06:21.07	−33.065	−70.161	112.1	7.4	1	21	4.4	71	35	0						
Dec. 4, 2001	09:09:47.20	−32.611	−39.665	135.2	13.2	1.2	22	4.1	20	81	−171						
Dec. 24, 2001	10:09:00.04	−33.636	−67.857	198.3	21.1	1.3	21	4.2				101	52	51			
Apr. 20, 2012	03:37:20.83	−34.370	−70.240	133.3	22.4	1.2	12	4.4	180	83	38	352	80	−17	350	88	−42
Aug. 22, 2012	16:33:06.79	−35.660	−70.050	163.3	17.1	0.7	9	2.1	18	28	−179	35	30	215	49	51	−147
June 6, 2013	17:42:16.68	−34.940	−69.500	166	4.1	0.1	6	3.5	185	69	78	162	90	80	176	69	77
Jan. 29, 2014	19:17:38.26	−35.510	−70.100	161	8.3	0.4	9	3.8	327	86	−114	309	11	62	140	83	134

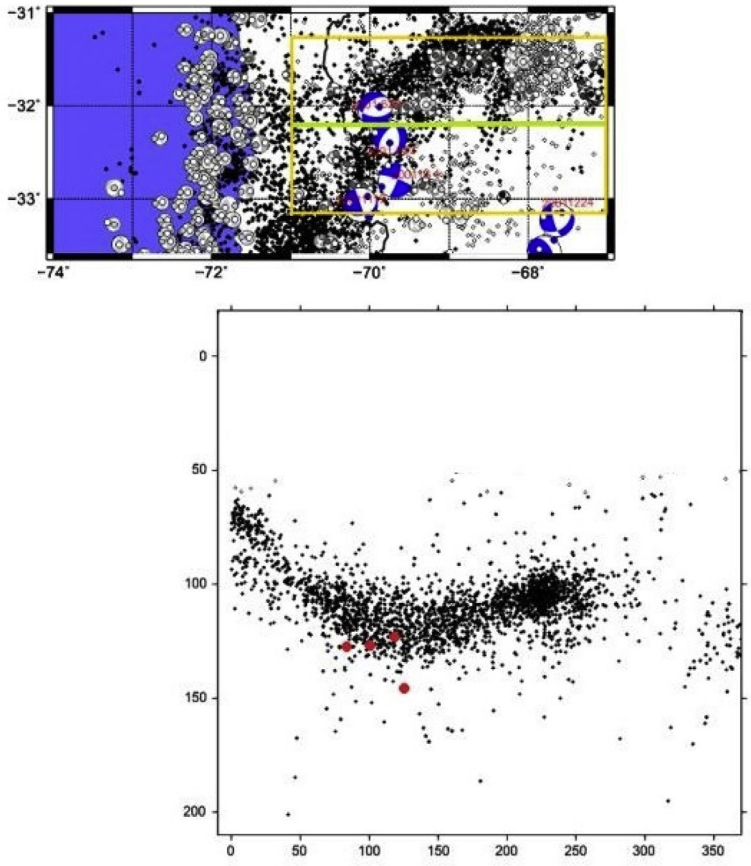

Fig. 5. NEIC/USGS catalog seismicity (black and white dots) and other earthquakes located in this work (red dots) along a profile at 32.2°S (green line).

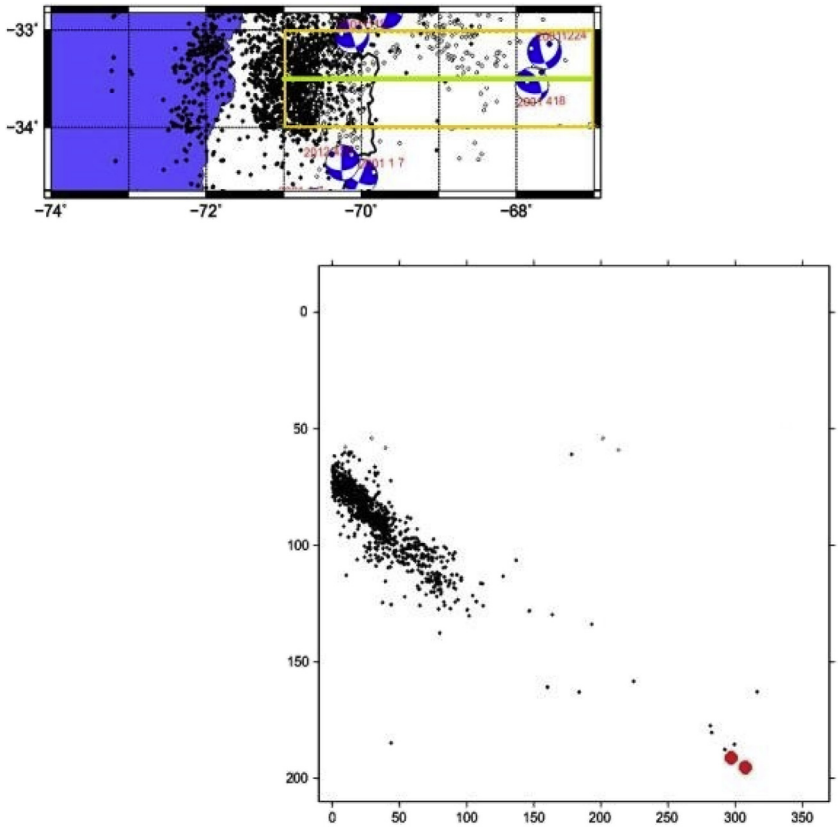

Fig. 6. NEIC/USGS catalog seismicity (black and white dots) and other earthquakes studied in this work (red dots) along a profile at 33.5°S (green line).

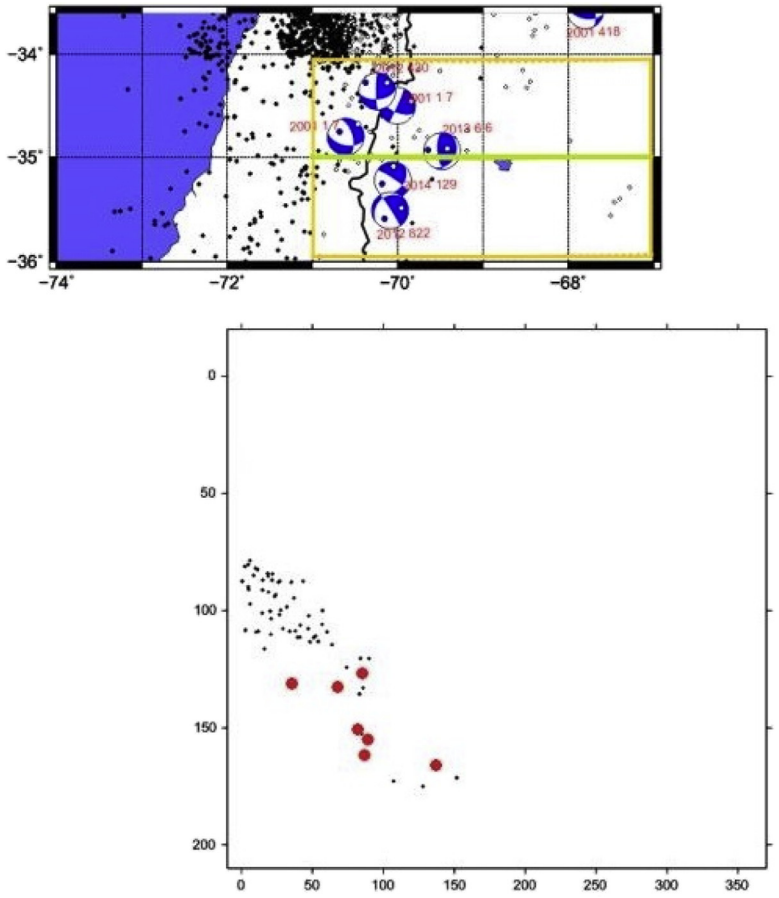

Fig. 7. NEIC/USGS catalog seismicity (black and white dots) and other earthquakes studied in this work (red dots) along a profile at 35°S (green line).

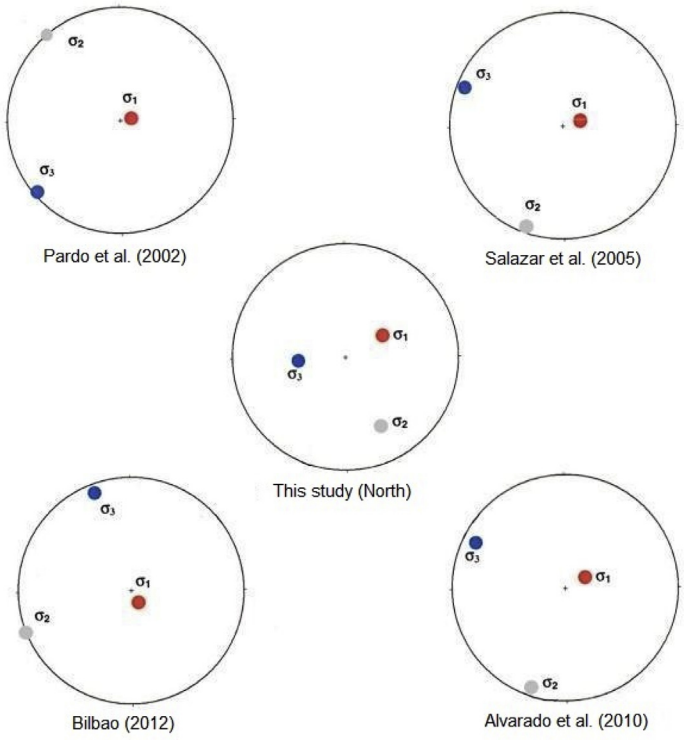

Fig. 8. Direction of the principal axes of stress tensor obtained in the northern zone of this study, compared to those obtained by other authors in the same area.

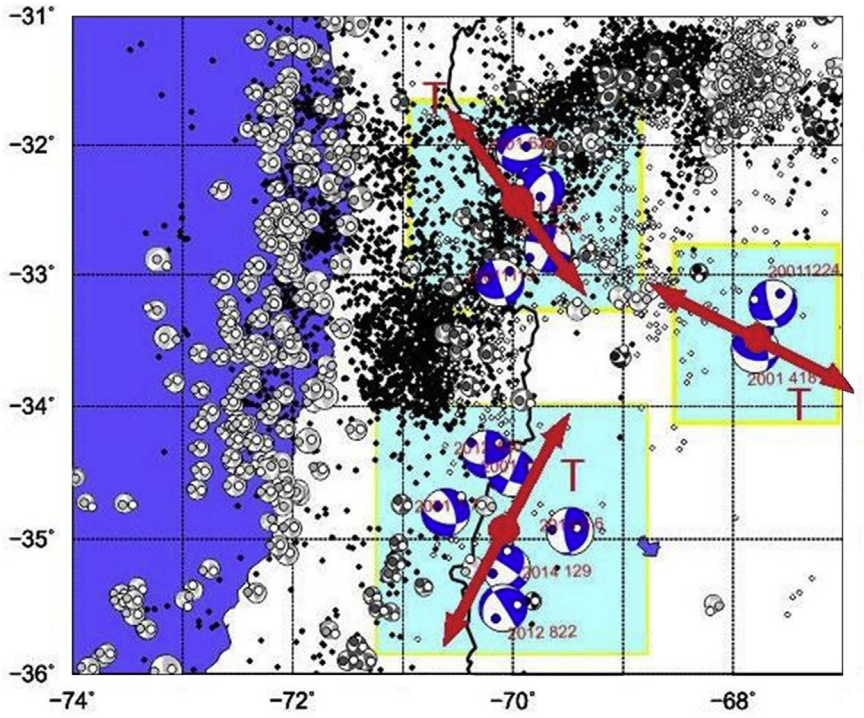

Fig. 9. Regional axes of minimum principal stress (T). All are oriented towards the center of the study area.

obtained with a strip of earthquakes in the west of the flat slab. This difference in earthquake selection criterions to obtain the regional tensor is responsible for these σ3 disagreements.

It was also found that the T axes of all the regions are oriented towards the central part of the study zone where the seismicity is very scarce (Fig. 9). This could indicate that in this area the slab is denser (eclogitized) and it would also explain the absence/scarcity of earthquakes in that sector. On the other hand, to the south, the existence of a plume pushing in the opposite direction to the slab pull force could counteract this force, even allow reverse and strike mechanisms by the twisting of the plate. It is noteworthy that the only mechanisms reported by CMT-NEIC at these depths and latitudes are a thrust solution in a region of typically normal earthquakes as well as the mechanism proposed in this study (2001/04/18). It is ruled out that these results are related to some transient phenomenon after the earthquake *M*w = 8.8 February 27, 2010 of Maule (Chile) since the formerly mentioned CMT mechanisms are previous. The gravimetric profile at 33.5°S is consistent with the conclusions obtained here, indicating the presence of a denser plate (eclogitized).

5. Conclusion

The Bouguer regional anomaly obtained in this work indicates the strong influence on gravity measurements of the Andean root.

The gravimetric model that best fits the observed data is consistent with a dense Nazca plate, which strengthens theories that affirm that it is totally or partially eclogitized at the latitudes analyzed.

The obtained results with the seismic and gravimetric techniques in this work were satisfactorily complemented.

The presence of seismic events at more than 190 km deep indicates that the Nazca plate continues to be present at these depths and contradicts theories that this could be broken at 33.5°S and longitudes around 68°W. Besides, the stress tensors suggest a denser plate, similar to that obtained with the gravimetric model. The locations of the events as well as their corresponding focal mechanisms are independent of the two velocity models used because such models do not differ for intermediate depths. Most of the focal mechanisms analyzed in this work are consistent in strike and dip to the outer rise faulting rotated at an angle equal to the subduction angle, therefore could be considered as reactivations of these.

Acknowledgments

The facilities of the IRIS Data Management System, and specifically the IRIS Data Management Center were used for access to waveform, metadata or products required in this study. Our research was funded by PICTO N°254 Riesgo Sísmico and PICT-2014-19 1697.

References

[1] E. Kendrick, M. Bevis, R. Smalley Jr., B. Brooks, R. Barriga Vargas, E. Lauría, et al., The Nazca – South America Euler vector and its rate of change, J S Am Earth Sci 16 (2003) 125–131.
[2] X. Tong, D. Sandwell, K. Luttrell, B. Brooks, M. Bevis, M. Shimada, et al., The 2010 Maule, Chile earthquake: downdip rupture limit revealed by space geodesy, Geophys Res Lett 38 (2011).
[3] C. Vigny, A. Socquet, S. Peyrat, J.-C. Ruegg, M. Métois, R. Madariaga, et al., The 2010 Mw 8.8 Maule megathrust earthquake of Central Chile, monitored by GPS, Science 332 (6036) (2011) 1417–1421, https://doi.org/10.1126/science.1204132, 17 Jun 2011.
[4] B. Delouis, J. Nocquet, M. Vallée, Slip distribution of the February 27, 2010 Mw = 8.8 Maule Earthquake, central Chile, from static and high-rate GPS,

InSAR, and broadband teleseismic data, Geophys Res Lett 37 (17) (2010), https://doi.org/10.1029/2010GL043899.
[5] M. Barazangi, B.L. Isacks, Spatial distribution of earthquakes and subduction of the Nazca plate beneath South America, Geology 4 (1976) 686–692.
[6] T.E. Jordan, B.L. Isacks, R.W. Allmendinger, J.A. Brewer, V.A. Ramos, C.J. Ando, Andean tectonics related to the geometry of the subducted Nazca plate, Geol Soc Am Bull 94 (1983) 341–361.
[7] T. Cahill, B.L. Isacks, Seismicity and shape of the subducted Nazca plate, J Geophys Res 97 (17) (1992) 503–529.
[8] M.L. Anderson, P. Alvarado, G. Zandt, S. Beck, Geometry and brittle deformation of the subducting Nazca Plate Central Chile and Argentina, Geophys J Int 171 (2007) 419–434.
[9] S. Nacif, E. Triep, S. Spagnotto, E. Aragon, R. Furlani, O. Álvarez, The flat to normal subduction transition study to obtain the Nazca plate morphology using high resolution seismicity data from the Nazca plate in Central Chile, Tectonophysics 657 (2015) (2015) 102–112.
[10] P. Mulcahy, C. Chen, S.M. Kay, L.D. Brown, B.L. Isacks, E. Sandvol, et al., Central Andean mantle and crustal seismicity beneath the Southern Puna plateau and the northern margin of the Chilean-Pampean flat slab, Tectonics 33 (2014) 1636–1658, https://doi.org/10.1002/2013TC003393.
[11] P. Kearey, A. Klepeis, F.J. Vine, Global tectonics, 3rd ed., Wiley-Blackwell, 2009, p. 496. ISBN: 978-1-4051-0777-8 Paperback.
[12] S.H. Kirby, E.R. Engdahl, R. Denlinger, Intermediate-depth intraslab earthquakes and arc volcanism as physical expressions of cristal and uppermost mantle metamorphism in subduction slabs, in: G.E. Bebout, D.W. Scholl, S.H. Kirby, J.P. Platt (Eds.), Subduction top bottom, American Geophisical Union, 1996, pp. 195–214. Geophysical Monograph, 96.
[13] C. Meade, R. Jeanloz, Deep focus earthquakes and recycling of water into the Earth's mantle, Science 252 (1991) 68–72.
[14] B.R. Hacker, S.M. Peacock, G.A. Abers, S.D. Holloway, Subduction factory, Are intermediate-depth earthquakes in subducting slabs linked to metamorphic dehydration reactions? J Geophys Res 108 (2003) https://doi.org/10.1029/2001JB001129.
[15] E. Contreras-Reyes, A. Osses, Lithospheric flexure modelling seaward of the Chile trench: implications for oceanic plate weakening in the trench outer rise region, Geophysics Journal International 182 (1) (2010) 97–112, https://doi.org/10.1111/j.1365-246X.2010.04629.x.
[16] W. Jiao, P.G. Silver, Y. Fei, C.T. Prewitt, Do intermediate- and deep-focus earthquakes occur on pre-existing weak zones? An examination of the Tonga subduction zone, J Geophys Res 105 (28) (2000) 125–138.
[17] C.R. Ranero, J.P. Morgan, K. McIntosh, C. Reichert, Bending-related faulting and mantle serpentinization at the Middle America trench, Nature 425 (2003) 367–373, https://doi.org/10.1038/nature01961.
[18] E. Contreras-Reyes, I. Grevemeyer, E.R. Flueh, C. Reichert, Upper lithospheric structure of the subduction zone offshore southern Arauco Peninsula, Chile at 38°S, J Geophys Res 113 (2008) B07303, https://doi.org/10.1029/2007JB005569.
[19] H. Kopp, E.R. Flueh, C. Papenberg, D. Klaeschen, Seismic investigations of the O'Higgins Seamount Group and Juan Fernández Ridge: aseismic ridge emplacement and lithosphere hydration, Tectonics 23 (2004), https://doi.org/10.1029/2003TCOO 1590.
[20] C.R. Gans, S.L. Beck, G. Zandt, H. Gilbert, P. Alvarado, M. Anderson, et al., Continental and oceanic crustal structure of the Pampean flat slab region, western Argentina, using receiver function analysis: new high-resolution results, J Geophys Res 186 (2011) 45–58, https://doi.org/10.1111/j.l365-246X.2011.05023.x.
[21] M. Pardo, D. Comte, T. Monfret, Seismotectonic and stress distribution in the central Chile subduction zone, J S Am Earth Sci 15 (2002) 11–22.
[22] S.I. Bilbao, Deformación sísmica de la placa de Nazca en las zonas adyascentes al segment de subducción horizontal (31°S) utilizando el modelado de ondas sísmicas regionales de banda ancha, Universidad Nacional de San Juan. Facultad de Cs. Es Físicas y Naturales, 2012. Tesis Doctoral.
[23] P. Salazar, Análisis del campo de esfuerzos en la zona de subducción bajo Chile central (30° – 34°S) [M.Sc.Thesis], Universidad de Chile, Santiago, Chile, 2005, p. 196.
[24] P. Alvarado, M. Pardo, H. Gilbert, S. Miranda, M. Anderson, M. Saez, et al., Flat-slab subduction and crustal models for the seismically active Sierras Pampeanas region of Argentina, in: S. Kay, V.A. Ramos, W. Dickinson (Eds.), MWR204: backbone of the Americas: shallow subduction, plateau uplift, and ridge and terrane collision, Geological Society of America, Boulder, Colorado, 2009, pp. 261–278.
[25] P. Alvarado, G. Sánchez, M. Saez, B. Castro de Machuca, Nuevas evidencias de la actividad sísmica del terreno Cuyania en la región de subducción de placa horizontal de Argentina, Rev Mex Ciencias Geol 27 (2) (2010) 278–291.
[26] S.V. Nacif, Sismotectónica de la placa de Nazca entre 33S y 35S por debajo de la zona sismogénica de interplacas y anisotropía sísmica en la corteza y manto superior de la placa suprayacente, Universidad Nacional de San Juan. Facultad de Ciencias Exactas, Físicas y Naturales. Instituto Geofísico Sismológico Volponi, 2012. Tesis doctoral.
[27] S.L. Spagnotto, Sismicidad entre 34.5°-36.5°S y 67°-71°O posterior al sismo de Maule, Mw=8.8, 27/02/2010 y distribuciones de deslizamientos en placa de Nazca para sismos de profundidades mayores a 100 km en secciones plana y normal entre 31-34°S, Universidad Nacional de San Juan. Facultad de Ciencias Exactas, Físicas y Naturales. Instituto Geofísico Sismológico Volponi, 2013. Tesis doctoral.
[28] S.L. Spagnotto, E.G. Triep, L.B. Giambiagi, S.V. Nacif, O. Alvarez, New evidences of rupture of crust and mantle in the subducted Nazca plate and intermediate-depth, J S Am Earth Sci. ISSN: 0895-9811 58 (2015) 141–147, https://doi.org/10.1016/j.jsames.2014.12.002. PII: S0895-9811(14)00167-9.
[29] A.I. Burd, J.R. Booker, R. Mackie, A. Favetto, M.C. Pomposiello, Three-dimensional electrical conductivity in the mantle beneath the Payún Matrú Volcanic Field in the Andean back-arc of Argentina near 36.5°S: decapitation of a mantle plume by resurgent upper mantle shear during slab steepening? Geophys J Int 198 (2) (2014) 812–827, https://doi.org/10.1093/gji/ggu145.
[30] A.I. Burd, J.R. Booker, M.C. Pomposiello, A. Favetto, J. Larsent, G. Giordanengo, et al., Electrical conductivity beneath the Payún Matrú volcanic field in the andean back-arc of Argentina near 36.5°S: insights into the magma source, in: 7th. International symposium on Andean geodynamics, Nice, France, Extended Abstracts, 2008, pp. 90–93.
[31] V.A. Ramos, A. Folguera, Payenia volcanic province in the Southern Andes: an appraisal of an exceptional quaternary tectonic setting, J Volcanol Geoth Res 201 (1–4) (2011) 53–64.
[32] M. Lupari, S. Spagnotto, S. Nacif, G. Yacante, H. Garcia, F. Linceklinger, M. Sanchez, E. Triep, Sismicidad Localizada en la Zona del Bloque San Rafael, Argentina, Rev Mex Ciencias Geol 32 (2015) 190–202.
[33] E.A. Rojas Vera, D. Sellés, A. Folguera, M. Gímenez, F. Ruíz, D. Orts, et al., The origin of the Loncopué Trough in the retroarc of the Southern Central Andes from field, geophysical and geochemical data, Tectonophysics (2014), https://doi.org/10.1016/j.tecto.2014.09.012.
[34] L. Ottemöller, P. Voss, J. Havskov, Seisan earthquake analysis software for windows, solaris, linux and macosx, 2011. http://seis.geus.net/software/seisan/seisan.html.
[35] J. Havskov, L. Ottemöller, R.L.P. Canabrava, SEISAN: multiplatform implementation of MINISEED/SEED, Orfeus Newslett 7 (2) (2007).
[36] J.L. Hardebeck, P.M. Shearer, A new method for determining first-motion focal mechanisms, Bull Seismol Soc Am 92 (2002) 2264–2276.
[37] J.A. Snoke, J.W. Munsey, A.G. Teague, G.A. Bollinger, A program for focal mechanism determination by combined used of polarity and SV-P amplitude ratio data, Earthq Notes 55 (1984) 15.
[38] P. Reasenberg, D. Oppenheimer, FPFIT, FPPLOT and FPPAGE: fortran computer programs for calculating and displaying earthquake fault-plane solutions, U.S. Geological Survey Open-File Report No. 85–739, 1985.
[39] C. Morelli, C. Gantar, T. Honkkasalon, K. McConnel, J.G. Tanner, B. Szabo, et al., The international gravity standardization Net 1971 (IGSN71), IUGG-IAG international union of geodesy and geophysics, Special Publication 4, Paris, 1974, p. 194.
[40] W.J. Hinze, Short note. Bouguer reduction density, why 2.67? Geophysics 68 (5) (2003) 1559–1560.
[41] M. Webring, SAKI: a FORTRAN program for generalized inversion of gravity and magnetic profiles, USGS Open File Report, 85–122, 1985, p. 29.
[42] A. Tassara, H.J. Gotze, S. Schmidt, R. Hackney, Three-dimensional density model of the Nazca plate and the Andean continental margin, J Geophys Res 111 (2006) B09404, https://doi.org/10.1029/2005JB003976.
[43] G.P. Woollard, Regional variations in gravity. The earth's crust and upper mantle. York, in: Pembroke J. Hart (Ed.), 1969, pp. 320–341.
[44] A. Introcaso, M.C. Pacino, F. Guspi, The Andes of Argentina and Chile: crustal configuration, isostasy, shortening and tectonic features from gravity data, Temas Geocienc 5 (2000) 31.
[45] M. Gimenez, P. Martinez, T. Jordan, F. Ruiz, F. Lince Klinger, Gravity characterization of the La Rioja Valley Basin, Argentina, Geophysics. ISSN: 00168033 74 (3) (2009) B83–B94.
[46] P. Martinez, M. Gimenez, A. Folguera, F. Lince Klinger, Integrated seismic and gravimetric model of Jocolí Basin. ISSN: 2324-8866, Interpretation, Argentina, 2014. T, 57–68.
[47] V.A. Ramos, Rasgos Estructurales del Territorio Argentino. Evolución tectónica de la Argentina. Geología Argentina. Editor Roberto Caminos, Anales 29 (24) (1999) 715–759.
[48] V.A. Ramos, Anatomy and global context of the Andes: main geologic features and the Andean orogenic cycle, Memoir 204, The Geological Society of America, 2009.
[49] M.P. Martinez, M. Gimenez, Fuerte anomalía gravimétrica Residual Positiva n el sistema de Famatina y su relación con paleosuturas. Explicaciones Alternativas, Asoc Geol Argent. ISSN: 0004-4822 58 (2) (2003) 176–186.
[50] M.C. Pacino, A. Introcaso, Modelo gravimétrico sobre el sistema de subducción Placa de Nazca Sudamericana en la latitud 33° Sur. V Congreso Geológico Chileno, T2., F, 77–89, 1988.
[51] J.D. Pesicek, E.R. Engdahl, C.H. Thurber, H.R. DeShon, D. Lange, Mantle subducting slab structure in the region of the 2010 M8.8 Maule earthquake (30–40°S), Chile, Geophys J Int 191 (2012) 317–324, https://doi.org/10.1111/j.1365-246X.2012.05624.x.

[52] S. Nacif, E. Triep, Incipiente zona de rotura en placa de Nazca subductada al sur de 33°S, XVIII Reunión Cientifica de la Asociación Argentina de Geofisicos y Geodestas y I Taller de Estaciones Continuas GNSS de America del Caribe, del 14 al 17 de Abril, Mendoza, Argentina, 2009.
[53] D. Portner, S. Beck, G. Zandt, A. Scire, The nature of sub-slab slow velocity anomalies beneath South America, American Geophysical Union, 2017.
[54] C.R. Ranero, A. Villaseñor, J. Phipps Morgan, W. Weinrebe, Relationship between bend-faulting at trenches and intermediate-depth seismicity, Geochem Geophys Geosyst 6 (2005) Q12002, https://doi.org/10.1029/2005GC000997.

Maria Lujan Eckerman, Bachelor in Geophysics, graduate in the Universidad Nacional del Sur (Argentina), specialized in Seismology. Current position: PhD student in Seismology at 31 Universidad Nacional de San Luis.